



Contents lists available at ScienceDirect

## Bioorganic &amp; Medicinal Chemistry

journal homepage: [www.elsevier.com/locate/bmc](http://www.elsevier.com/locate/bmc)

## Dual inhibitors of the human blood-brain barrier drug efflux transporters P-glycoprotein and ABCG2 based on the antiviral azidothymidine

Hilda A. Namanja-Magliano, Kelsey Bohn, Neha Agrawal, Meghan E. Willoughby, Christine A. Hrycyna, Jean Chmielewski\*

Department of Chemistry, Purdue University, 560 Oval Drive, West Lafayette, IN 47907-2084, USA

## ARTICLE INFO

## Article history:

Received 8 May 2017  
Revised 29 June 2017  
Accepted 2 July 2017  
Available online xxxxx

## Keywords:

Blood-brain barrier  
P-glycoprotein  
ABCG2  
AZT  
Inhibition

## ABSTRACT

The brain provides a sanctuary site for HIV due, in part, to poor penetration of antiretroviral agents at the blood-brain barrier. This lack of penetration is partially attributed to drug efflux transporters such as P-glycoprotein (P-gp) and ABCG2. Inhibition of both ABCG2 and P-gp is critical for enhancing drug accumulation into the brain. In this work, we have developed a class of homodimers based on the HIV reverse transcriptase inhibitor azidothymidine (AZT) that effectively inhibits P-gp and ABCG2. These agents block transporter mediated efflux of the P-gp substrate calcein-AM and the ABCG2 substrate mitoxantrone. The homodimers function by interacting with the transporter drug binding sites as demonstrated by competition studies with the photo-affinity agent and P-gp/ABCG2 substrate [<sup>125</sup>I]iodoarylazidoprazosin. As such, these dual inhibitors of both efflux transporters provide a model for the future development of delivery vehicles for antiretroviral agents to the brain.

© 2017 Elsevier Ltd. All rights reserved.

### 1. Introduction

Highly active antiretroviral therapy (HAART) is a combination of several antiretroviral agents that target the different stages in the viral life cycle, and is the standard HIV treatment for patients. This multidrug approach has been very successful in reducing viral loads and patient mortality.<sup>1</sup> However, HIV eradication is a significant challenge because reservoirs persist in cellular and anatomical locations, such as the brain.<sup>2</sup> HIV reservoirs in the brain have been attributed, in part, to poor penetration of antiretroviral agents at the blood-brain barrier (BBB). ATP binding cassette transporters at the BBB, such as P-glycoprotein (P-gp) and the ABCG2 play a part in limiting drug accumulation in the brain that results in suboptimal drug levels.<sup>3-6</sup>

P-gp and ABCG2 are expressed at the luminal membrane of brain capillary endothelial cells where they efflux a range of substrates from the cell.<sup>7-9</sup> A number of antiretroviral drugs, including HIV protease inhibitors<sup>10-12</sup> and reverse transcriptase inhibitors, such as abacavir and AZT<sup>13,14</sup> are substrates of P-gp. The effect of ABCG2 on AZT bioavailability has also been studied in *in vitro* models.<sup>15,16</sup> For example, ABCG2 limited the antiviral activity of AZT in

CD4<sup>+</sup> T cells highly expressing ABCG2 as compared to wild-type cells.<sup>16</sup> These data demonstrate that there is an acute need for modulators of the drug efflux pumps at the BBB for co-administration with HIV therapeutics.

We have recently reported a series of prodrug dimeric abacavir inhibitors that target the drug binding sites of P-gp.<sup>17</sup> However, drugs such as AZT are recognized by both P-gp and ABCG2. Thus blocking only one of these transporters would still allow for efflux by the other. Therefore, it is essential to generate agents that can simultaneously inhibit both proteins. In this study, we disclose a class of AZT dimers that prevent substrate efflux by both P-gp and ABCG2. In a proof of concept study, we demonstrate that the AZT dimers compete with substrate binding sites that are located in the transmembrane region of both transporters.

### 2. Experimental section

#### 2.1. Materials

AZT and 1-ethyl-3-(3-dimethylaminopropyl)carbodiimide (EDC) were purchased from AK Scientific (Union City, CA). 4-dimethylaminopyridine (DMAP) was purchased from GenScript (Piscataway, NJ). Calcein-AM was obtained from Invitrogen (Carlsbad, CA). [<sup>125</sup>I]-iodoarylazidoprazosin ([<sup>125</sup>I]-IAAP) was

\* Corresponding author.

E-mail address: [chml@purdue.edu](mailto:chml@purdue.edu) (J. Chmielewski).

purchased from Pelkin Elmer (Waltham, MA) and all other reagents were obtained from Sigma-Aldrich (St. Louis, MO).

## 2.2. Methods

### 2.2.1. General synthesis of AZT dimers

To a solution of commercially available dicarboxylic acids (0.125 mmol) in dry dimethylformamide (DMF) (1.5 mL) at 0 °C was added EDC (0.374 mmol), DMAP (0.062 mmol), and diisopropylethyl amine (DIEA) (0.744 mmol). After 20 min at 0 °C, AZT (0.374 mmol) dissolved in DMF (500 µL) was added. The mixture was allowed to warm to room temperature and stirred for 12 h. The solvent was removed *in vacuo*. The resulting crude mixtures of **AZT-C2** and **AZT-C5** were purified by silica gel flash column chromatography to obtain the pure products **AZT-C2** (28% yield), **AZT-C5** (45% yield). The dimers **AZT-C8**, **AZT-C10** and **AZT-C12** were purified to homogeneity by reverse-phase (RP) HPLC using a semi-preparative C5 column (Phenomenex, USA). The eluent consisted of solvent A (H<sub>2</sub>O/0.1% trifluoroacetic acid (TFA)) and solvent B (methanol/0.1%TFA) over a 60 min gradient consisting of 20–95% solvent B, with a flow rate of 10 mL/min, and UV detection at 214. The desired compounds were lyophilized to obtain **AZT-C8** (40% yield), **AZT-C10** (42% yield) and **AZT-C12** (61% yield). The compounds were characterized by ESI mass spectrometry (Table 1) and NMR, and the purity (>98%) was confirmed by analytical RP HPLC (Table 1).

**AZT-C2:** <sup>1</sup>H NMR (500 MHz, DMSO-*d*<sub>6</sub>) δ 11.34 (s, 2H), 7.44 (d, *J* = 1.1 Hz, 2H), 6.11 (t, *J* = 6.5 Hz, 2H), 4.43 (dt, *J* = 7.5, 5.9 Hz, 2H), 4.29–4.20 (m, 4H), 3.97–3.91 (m, 2H), 2.68–2.58 (m, 4H), 2.47–2.39 (m, 2H), 2.35–2.28 (m, 2H), 1.78 (d, *J* = 1.0 Hz, 6H); <sup>13</sup>C NMR (126 MHz, DMSO-*d*<sub>6</sub>) 172.2, 164.1, 150.8, 136.4, 110.4, 84.0, 81.0, 63.9, 60.4, 36.0, 28.9, 12.5.

**AZT-C5:** <sup>1</sup>H NMR (500 MHz, DMSO-*d*<sub>6</sub>) δ 11.34 (s, 2H), 7.45–7.42 (m, 2H), 6.10 (t, *J* = 6.5 Hz, 2H), 4.47–4.37 (m, 2H), 4.27–4.18 (m, 4H), 3.98–3.93 (m, 2H), 2.47–2.40 (m, 2H), 2.39–2.26 (m, 6H), 1.79–1.77 (m, 6H), 1.51 (p, *J* = 7.5 Hz, 4H), 1.30–1.20 (m, 2H); <sup>13</sup>C NMR (126 MHz, DMSO-*d*<sub>6</sub>) 173.0, 164.1, 150.8, 136.5, 110.3, 84.0, 81.0, 63.6, 60.6, 36.1, 33.6, 28.3, 24.4, 12.6.

**AZT-C8:** <sup>1</sup>H NMR (500 MHz, DMSO-*d*<sub>6</sub>) δ 11.34 (s, 2H), 7.44 (d, *J* = 1.1 Hz, 2H), 6.14–6.08 (m, 2H), 4.44 (dt, *J* = 7.5, 5.8 Hz, 2H), 4.30–4.17 (m, 4H), 3.98–3.93 (m, 2H), 2.47–2.40 (m, 2H), 2.38–2.25 (m, 6H), 1.78 (d, *J* = 0.9 Hz, 6H), 1.56–1.43 (m, 4H), 1.27–1.18 (m, 8 H); <sup>13</sup>C NMR (126 MHz, DMSO-*d*<sub>6</sub>) 173.1, 164.1, 150.8, 136.5, 110.3, 84.0, 81.0, 63.5, 60.6, 36.1, 33.8, 28.9, 28.8, 24.7, 12.6.

**AZT-C10:** <sup>1</sup>H NMR (500 MHz, DMSO-*d*<sub>6</sub>) δ 11.34 (s, 2H), 7.44–7.73 (m, 2H), 6.11 (t, *J* = 6.5 Hz, 2H), 4.44 (dt, *J* = 7.4, 5.8 Hz, 2H), 4.28–4.20 (m, 4H), 3.98–3.93 (m, 2H), 2.47–2.39 (m, 2H), 2.37–2.26 (m, 6H), 1.78 (d, *J* = 0.9 Hz, 6H), 1.54–1.41 (m, 4H), 1.26–1.18 (m, 12 H); <sup>13</sup>C NMR (126 MHz, DMSO-*d*<sub>6</sub>) 173.1, 164.1, 150.8, 136.5, 110.3, 84.0, 81.0, 63.5, 60.6, 36.1, 33.8, 29.2, 29.1, 28.8, 24.8, 12.6.

**AZT-C12:** <sup>1</sup>H NMR (500 MHz, DMSO-*d*<sub>6</sub>) δ 11.34 (s, 2H), 7.43 (d, *J* = 1.1 Hz, 2H), 6.11 (t, *J* = 6.5 Hz, 2H), 4.47–4.40 (m, 2H), 4.29–4.18 (m, 4H), 3.98–3.93 (m, 2H), 2.47–2.39 (m, 2H), 2.37–2.26 (m, 6H),

1.82–1.72 (m, 6H), 1.54–1.46 (m, 4H), 1.27–1.18 (m, 16H); <sup>13</sup>C NMR (126 MHz, DMSO-*d*<sub>6</sub>) 173.1, 164.1, 150.8, 136.4, 110.3, 84.0, 81.0, 63.5, 60.6, 36.1, 33.8, 29.4, 29.30, 29.1, 28.9, 24.8, 12.6.

### 2.2.2. Cell culture

MCF-7 cells (breast adenocarcinoma) were cultured in RPMI 1640 supplemented with 2 mM L-glutamine, 50 µg/mL streptomycin (Cellgro Mediatech, Herndon, VA), 50 units/mL of penicillin and 10% fetal bovine serum (FBS) (Cambrex bioscience, Walkersville, Inc) at 37 °C in 5% CO<sub>2</sub>. MCF-7/FLV1000 cells (breast adenocarcinoma over-expressing BCRP) were cultured in RPMI 1640 medium supplemented with 10% fetal bovine serum FBS, 2 mM L-glutamine, 50 units/mL penicillin, 50 µg/mL streptomycin (Mediatech), and 1000 nM flavopiridol (NIH AIDS Reagent program, Germantown, MD).

MCF-7/DX1 cells (breast adenocarcinoma over-expressing P-gp) were maintained in RPMI 1640 supplemented with 2 mM L-glutamine, 50 µg/mL streptomycin, 50 units/mL of penicillin, 10% fetal bovine serum and 1 µM doxorubicin (TCI America).

Sf9 cells were cultured at 27 °C in SF-900 II SFM medium (Invitrogen) supplemented with 0.5X antibiotic-antimycotic (Invitrogen).

### 2.2.3. Flow cytometry assays

Flow cytometry assays were performed as described previously with minor modifications.<sup>18</sup> For P-gp experiments: an aliquot of the substrate fluorophore, calcein-AM dissolved in DMSO was added to pre-warmed basal medium eagle (BME) media to give a final concentration of 0.5 µM. The fluorophore treated BME media (1 mL) was incubated with 125,000 MCF-7/DX1 cells (in suspension) in the presence of increasing concentrations of the compounds of interest at 37 °C for 10 min, keeping the concentration of the vehicle for the compounds (DMSO) constant at 5%, a value in which the cells were fully viable during the course of the experiment. GF120918 (1 µM) (P-gp and ABCG2 inhibitor) was used as a positive control. Cells were collected by centrifugation and resuspended in ice cold phosphate buffered saline (PBS, pH 7.4). The cells were analyzed for fluorescent substrate accumulation using a FACSCalibur flow cytometer (BD Biosciences, San Jose, CA) equipped with a 488 nm argon laser and a 530 nm band pass filter (FL1). Ten thousand cells were counted for each data point and the mean fluorescence was used to determine the IC<sub>50</sub> values using GraphPad Prism 4. All experiments were performed in triplicate.

For ABCG2 experiments an aliquot of the substrate fluorophore, mitoxantrone, dissolved in DMSO was added to pre-warmed basal medium eagle (BME) media to give a final concentration of 20 µM. The fluorophore treated BME media (1 mL) was incubated with 125,000 MCF-7/FLV1000 cells (in suspension) in the presence of increasing concentrations of the compounds of interest at 37 °C for 30 min, keeping the concentration of the vehicle for the compounds (DMSO) constant at 2%. GF120918 (2 µM) was used as a positive control. Cells were harvested by centrifugation and re-suspended in 1 mL BME media containing either 2 µM GF120918 or increasing concentrations of the compounds of

**Table 1**  
Characterization of AZT dimers.

Compound	HPLC Conditions <sup>a</sup>	Retention Time (min)	MS Calculated	ESI-MS Observed
<b>AZT-C2</b>	5–95% B <sup>b</sup>	14.6	616.54	617.09
<b>AZT-C5</b>	5–95% B <sup>b</sup>	16.8	658.62	659.09
<b>AZT-C8</b>	5–95% B <sup>b</sup>	19.1	700.70	701.10
<b>AZT-C10</b>	5–95% B <sup>b</sup>	20.5	728.75	729.21
<b>AZT-C12</b>	5–95% B <sup>b</sup>	21.9	756.81	757.09

<sup>a</sup> 1.2 mL/min flow rate.

<sup>b</sup> Solvent A: H<sub>2</sub>O/0.05% TFA and B: acetonitrile /0.05%TFA.

interest, and incubated another 30 min at 37 °C to allow transporter-mediated efflux. These cells were collected by centrifugation at 300×g, re-suspended in ice cold phosphate buffered saline (PBS), pH 7.4, and analyzed using a FACSCalibur flow cytometer (BD Biosciences, San Jose, CA) equipped with a 488 nm argon laser and a 670 nm band pass filter (FL3). All experiments were performed in triplicate.

### 2.2.4. Preparation of P-gp and ABCG2 membranes

BV-MDR1 (baculovirus-MDR1) for BV-ABCG2 (baculovirus-ABCG2) infected Sf9 cells were collected and crude membrane extracts prepared as described previously.<sup>19</sup> P-gp expression was verified by immunoblot with C219 primary antibody (1:8000) and HRP-conjugated anti-mouse secondary antibody (1:8000) while ABCG2 expression was verified by immunoblot with BXP21 primary antibody (1:8000) and HRP-conjugated antimouse secondary antibody (1:8000).

### 2.2.5. Photo-affinity labeling with [<sup>125</sup>I]-IAAP

Photoaffinity labeling was performed as previously described with minor modifications.<sup>18</sup> Crude Sf9 membranes expressing P-gp (25 µg) or BCRP (40 µg) were incubated for 10 min at room temperature in the dark in Tris buffer (50 mM; pH 7.5), 1% aprotinin, 1 mM DTT, and 2 mM 4-(2-aminoethyl) benzenesulfonyl fluoride hydrochloride with either 2.5% DMSO (negative control) or GF120918 (positive control) dissolved in DMSO (to give a final concentration of 10 µM for P-gp experiments and 20 µM for ABCG2 experiments) or increasing concentrations of the compounds of interest (dissolved in DMSO) and [<sup>125</sup>I]-IAAP (1 µL, specific activity of ~2200 Ci/mmol). The samples were illuminated with UV light (365 nm) for 20 min on ice. 5X Laemmli SDS sample buffer was added to a final concentration of 2X and the samples were incubated at room temperature for 30 min. Proteins were then separated by SDS-PAGE (7.5% Tris gel). The gel was fixed and allowed to dry overnight and exposed to X-ray film at –80 °C. The gel band corresponding to P-gp or BCRP was analyzed using ImageJ (NIH) to determine the amount of [<sup>125</sup>I]-IAAP photocrosslinked to P-gp or BCRP. Values are represented as a percent of the DMSO control sample, and the IC<sub>50</sub> values were determined by GraphPad Prism 4.

### 2.2.6. Cell viability assays

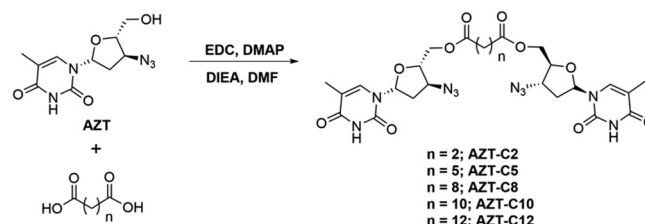
Cell viability was measured using a standard MTT assay after 24 h in the presence of increasing concentrations of dimers with MCF-7/FLV1000 and MCF-7/DX1 cells. Cell viability was calculated as a ratio of absorbance of the cells treated with the library compounds relative to untreated cells.

## 3. Results and discussion

### 3.1. Design and synthesis of AZT homodimers

Studies have shown that P-gp contains multiple binding sites, where two or more substrates can bind simultaneously.<sup>20–25</sup> Using this feature to our advantage, we have previously converted several therapeutic substrates of P-gp into dimers that inhibit the transporter.<sup>17,26–31</sup> We thus used this strategy to generate a total of five homodimers of AZT with varying lengths of methylene-based linkers (**AZT-C2–AZT-C12**) (Scheme 1). We hypothesized that such a library of dimers with different tether lengths would allow us to probe the distance between AZT binding sites on P-gp.

Since AZT is also a substrate of ABCG2, we wanted to explore AZT dimers as inhibitors of this transporter as well. Compared to P-gp which functions as a monomer, ABCG2 is a “half transporter” that dimerizes to form the active transporter.<sup>32,33</sup> Given its overall homology and overlapping substrate specificities with P-gp, ABCG2



Scheme 1. Synthesis of AZT dimers.

is also proposed to have multiple binding sites that are formed through homodimeric assembly. As such, we hypothesized that AZT dimers may also inhibit ABCG2.

AZT contains a primary alcohol which we used successfully to form ester-linked dimers with varying length tethers (Scheme 1). The dimers were synthesized by activating the appropriate dicarboxylic acids with EDC, followed by the addition of AZT in the presence of catalytic DMAP and DIEA (Scheme 1). The resulting dimers were purified to homogeneity and characterized by mass spectrometry (Table 1).

### 3.2. Dimers inhibit P-gp and ABCG2 in cultured cells with minimal toxicity

The inhibitory potency of the dimers towards both transporters was evaluated using human carcinoma cell lines that overexpress P-gp (MCF-7/DX1) and ABCG2 (MCF-7/FLV1000). The P-gp substrate calcein-AM was used in a fluorescence accumulation flow cytometry assay to assess the effect of the dimers **AZT-C2** through **AZT-C12** and the AZT monomer on P-gp transport. Once inside cells calcein-AM is cleaved by esterases yielding fluorescent calcein. In this assay, substrates of P-gp do not accumulate within cells and fluorescence, therefore, is not observed. However, inhibition of P-gp leads to accumulation of the substrate within the cells and a resulting increase in cellular fluorescence. In the case of AZT, addition of up to 500 µM of the monomer to MCF-7/DX1 cells did not increase the accumulation of calcein in the P-gp expressing cells, indicating no inhibition of P-gp (Table 2). The dimers with shortest lengths, **AZT-C2** and **AZT-C5**, displayed negligible inhibition of P-gp transport at concentrations greater than 200 µM. As the tether length was increased, however, the dimer activity also increased, with **AZT-C10** and **AZT-C12** displaying about 5-fold greater inhibition as compared to **AZT-C8** (Table 2).

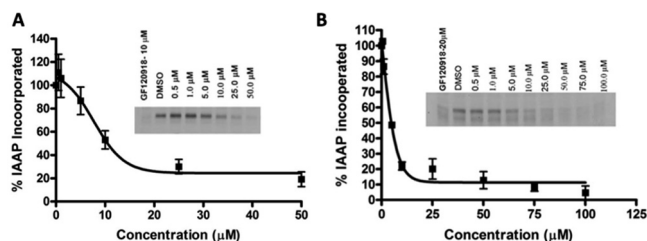
We used a human breast carcinoma cell line over-expressing ABCG2 (MCF-7/FLV1000) to evaluate the inhibitory efficacy of the AZT dimers. Fluorescent substrate accumulation assays with AZT-dimers were performed with the ABCG2 substrate mitoxantrone (Table 2). These data indicate that AZT dimers with longer tethers were the most effective as inhibitors of the transporter. For example, **AZT-C8**, **AZT-C10** and **AZT-C12** were notably more potent as compared **AZT-C2** and **AZT-C5**, whereas the AZT monomer did not inhibit ABCG2 up to 400 µM (Table 2). Interestingly, these data

Table 2

Effect of AZT and AZT dimers on P-gp mediated efflux of calcein-AM and ABCG2-mediated efflux of mitoxantrone.

Compound	P-gp Inhibition IC <sub>50</sub> (µM)	ABCG2 Inhibition IC <sub>50</sub> (µM)
<b>AZT</b>	NI <sup>a</sup> up to 500	NI <sup>a</sup> up to 400
<b>AZT-C2</b>	NI <sup>a</sup> up to 400	NI <sup>a</sup> up to 200
<b>AZT-C5</b>	>200	NI <sup>a</sup> up to 200
<b>AZT-C8</b>	11.3 ± 0.7	28.2 ± 0.4
<b>AZT-C10</b>	2.3 ± 0.1	11.5 ± 3.6
<b>AZT-C12</b>	2.0 ± 0.03	13.3 ± 2.2

<sup>a</sup> NI = no inhibition.



**Fig. 1.** Competition between **AZT-C10** and [<sup>125</sup>I]-IAAP for binding sites on (A) P-gp and (B) ABCG2. DMSO was used as the negative control and GF120918 as the positive control.

were similar to the P-gp inhibition data. The similarity in these trends described above suggests that the distance between binding sites in ABCG2 is similar to the sites in P-gp.

### 3.3. AZT dimers inhibit P-gp and ABCG2 by competing for substrate binding sites

Thus far, we have shown that the longer tether length AZT dimers inhibit P-gp and ABCG2, but have not demonstrated the mechanism of inhibition. Since, the AZT dimers were designed to interact with the substrate binding sites of the transporters, they should compete with substrates for these sites. To confirm that the AZT dimers bind to the substrate binding sites, competition studies were conducted with the [<sup>125</sup>I]-radiolabeled azido-analog of prazosin [<sup>125</sup>I]-IAAP (Fig. 1). Prazosin is a known substrate of both P-gp<sup>20</sup> and ABCG2.<sup>34</sup> Furthermore, [<sup>125</sup>I]-IAAP is known to bind to P-gp at sites localized to the transmembrane domain of the transporter.<sup>35</sup> In these experiments, **AZT-C10** was used because it is a potent inhibitor of both transporters. Sf9 insect membranes that expressed P-gp or ABCG2 were incubated with **AZT-C10** and [<sup>125</sup>I] IAAP, followed by photocrosslinking. After SDS-PAGE, the intensity of the radiolabeled bands from [<sup>125</sup>I] IAAP and P-gp or ABCG2 were quantitated by densitometry using ImageJ. **AZT-C10** competed with [<sup>125</sup>I] IAAP for binding to both P-gp (Fig. 1A) and ABCG2 (Fig. 1B) in a concentration dependent manner, with an IC<sub>50</sub> values of 9.3 ± 2.3 µM and 4.3 ± 0.7 µM, respectively. These data suggest that the AZT-dimer inhibits the transporters by competing for the prazosin binding sites in the transmembrane domains.

Importantly, using a standard MTT assay,<sup>36</sup> we determined that our most potent dimers in the library, **AZT-C10** and **AZT-C12**, showed minimal toxicity (>95% viability) to both the MCF-7/DX1 and MCF-7/FLV1000 cell lines at the concentrations required for inhibition of both P-gp and ABCG2. The only exception was **AZT-C12** with MCF-7/FLV1000 cells which demonstrated approximately 60% viability at 40 µM.

## 4. Conclusions

Expression P-gp and ABCG2 at the BBB play a pivotal role in limiting brain levels of antiretroviral agents, such as AZT. Thus, in this proof of concept study, we synthesized AZT-based homodimers with the goal of inhibiting these transporters. A library of dimers with varied in tether lengths was prepared. Of these, the longer tether lengths afforded more potent inhibitors of both P-gp and ABCG2 in mammalian cell lines. Competition experiments with the photo-affinity substrate [<sup>125</sup>I]-IAAP also demonstrated that these dimers compete with substrates for transporter binding. Taken together, these data suggest that the dimers serve as competitive inhibitors. Given that a number of antiretroviral agents are substrates for both proteins, these agents have potential to provide enhanced delivery of the antiretrovirals across the BBB.

## Acknowledgements

We acknowledge financial support from the National Institutes of Health.

## A. Supplementary data

Supplementary data associated with this article can be found, in the online version, at <http://dx.doi.org/10.1016/j.bmc.2017.07.001>.

## References

- Blankson JN, Persaud D, Siliciano RF. The challenge of viral reservoirs in HIV-1 infection. *Annu Rev Med.* 2002;53:557–593.
- Schrager LK, D'Souza MP. Cellular and anatomical reservoirs of HIV-1 in patients receiving potent antiretroviral combination therapy. *JAMA.* 1998;280:67–71.
- Varatharajan L, Thomas SA. The transport of anti-HIV drugs across blood-CNS interfaces: summary of current knowledge and recommendations for further research. *Antiviral Res.* 2009;82:A99–109.
- Schinkel AH, Jonker JW. Mammalian drug efflux transporters of the ATP binding cassette (ABC) family: an overview. *Adv Drug Deliv Rev.* 2003;55:3–29.
- Linton KJ. Structure and function of ABC transporters. *Physiology (Bethesda).* 2007;22:122–130.
- Loscher W, Potschka H. Drug resistance in brain diseases and the role of drug efflux transporters. *Nat Rev Neurosci.* 2005;6:591–602.
- Cordon-Cardo C, O'Brien JP, Casals D, et al. Multidrug-resistance gene (P-glycoprotein) is expressed by endothelial cells at blood-brain barrier sites. *Proc Natl Acad Sci U S A.* 1989;86:695–698.
- Jette L, Tetu B, Beliveau R. High levels of P-glycoprotein detected in isolated brain capillaries. *Biochim Biophys Acta.* 1993;1150:147–154.
- van Herwaarden AE, Schinkel AH. The function of breast cancer resistance protein in epithelial barriers, stem cells and milk secretion of drugs and xenotoxins. *Trends Pharmacol Sci.* 2006;27:10–16.
- Lee CG, Gottesman MM, Cardarelli CO, et al. HIV-1 protease inhibitors are substrates for the MDR1 multidrug transporter. *Biochemistry.* 1998;37:3594–3601.
- Kim RB, Fromm MF, Wandel C, et al. The drug transporter P-glycoprotein limits oral absorption and brain entry of HIV-1 protease inhibitors. *J Clin Invest.* 1998;101:289–294.
- Choo EF, Leake B, Wandel C, et al. Pharmacological inhibition of P-glycoprotein transport enhances the distribution of HIV-1 protease inhibitors into brain and testes. *Drug Metab Dispos.* 2000;28:655–660.
- Shaik N, Giri N, Pan G, Elmquist WF. P-glycoprotein-mediated active efflux of the anti-HIV-1 nucleoside abacavir limits cellular accumulation and brain distribution. *Drug Metab Dispos.* 2007;35:2076–2085.
- Quevedo MA, Nieto LE, Brinon MC. P-glycoprotein limits the absorption of the anti-HIV drug zidovudine through rat intestinal segments. *Eur J Pharm Sci.* 2011;43:151–159.
- Pan G, Giri N, Elmquist WF. Abcg2/Bcrp1 mediates the polarized transport of antiretroviral nucleosides abacavir and zidovudine. *Drug Metab Dispos.* 2007;35:1165–1173.
- Wang X, Nitanda T, Shi M, et al. Induction of cellular resistance to nucleoside reverse transcriptase inhibitors by the wild-type breast cancer resistance protein. *Biochem Pharmacol.* 2004;68:1363–1370.
- Namanja HA, Emmert D, Davis DA, et al. Toward eradicating HIV reservoirs in the brain: inhibiting P-glycoprotein at the blood-brain barrier with prodrug abacavir dimers. *J Am Chem Soc.* 2012;134:2976–2980.
- Hrycyna CA, Ramachandra M, Pastan I, Gottesman MM. Functional expression of human P-glycoprotein from plasmids using vaccinia virus-bacteriophage T7 RNA polymerase system. *Methods Enzymol.* 1998;292:456–473.
- Germann UA, Willingham MC, Pastan I, Gottesman MM. Expression of the human multidrug transporter in insect cells by a recombinant baculovirus. *Biochemistry.* 1990;29:2295–2303.
- Dey S, Ramachandra M, Pastan I, Gottesman MM, Ambudkar SV. Evidence for two nonidentical drug-interaction sites in the human P-glycoprotein. *Proc Natl Acad Sci U S A.* 1997;94:10594–10599.
- Bruggemann EP, Currier SJ, Gottesman MM, Pastan I. Characterization of the azidopine and vinblastine binding site of P-glycoprotein. *J Biol Chem.* 1992;267:21020–21026.
- Loo TW, Bartlett MC, Clarke DM. Simultaneous binding of two different drugs in the binding pocket of the human multidrug resistance P-glycoprotein. *J Biol Chem.* 2003;278:39706–39710.
- Martin C, Berridge G, Higgins CF, et al. Communication between multiple drug binding sites on P-glycoprotein. *Mol Pharmacol.* 2000;58:624–632.
- Aller SG, Yu J, Ward A, et al. Structure of P-glycoprotein reveals a molecular basis for poly-specific drug binding. *Science.* 2009;323:1718–1722.
- Shapiro AB, Ling V. Positively cooperative sites for drug transport by P-glycoprotein with distinct drug specificities. *Eur J Biochem.* 1997;250:130–137.
- Pires MM, Emmert D, Hrycyna CA, Chmielewski J. Inhibition of P-glycoprotein-mediated paclitaxel resistance by reversibly linked quinine homodimers. *Mol Pharmacol.* 2009;75:92–100.

27. Pires MM, Hrycyna CA, Chmielewski J. Bivalent probes of the human multidrug transporter P-glycoprotein. *Biochemistry*. 2006;45:11695–11702.
28. Kuriakose J, Hrycyna CA, Chmielewski J. Click chemistry-derived bivalent quinine inhibitors of P-glycoprotein-mediated cellular efflux. *Bioorg Med Chem Lett*. 2012;22:4410–4412.
29. Namanja HA, Emmert D, Hrycyna CA, Chmielewski J. Homodimers of the antiviral abacavir as modulators of P-glycoprotein transport in cell culture: probing tether length. *Med Chem Comm*. 2013;4:1344–1349.
30. Emmert D, Campos CR, Ward D, et al. Reversible dimers of the atypical antipsychotic quetiapine inhibit p-glycoprotein-mediated efflux in vitro with increased binding affinity and in situ at the blood-brain barrier. *ACS Chem Neurosci*. 2014;5:305–317.
31. Sauna ZE, Andrus MB, Turner TM, Ambudkar SV. Biochemical basis of polyvalency as a strategy for enhancing the efficacy of P-glycoprotein (ABCG1) modulators: Stipiamide homodimers separated with defined-length spacers reverse drug efflux with greater efficacy. *Biochemistry*. 2004;43:2262–2271.
32. McDevitt CA, Collins RF, Conway M, et al. Purification and 3D structural analysis of oligomeric human multidrug transporter ABCG2. *Structure*. 2006;14:1623–1632.
33. Bhatia A, Schafer HJ, Hrycyna CA. Oligomerization of the human ABC transporter ABCG2: evaluation of the native protein and chimeric dimers. *Biochemistry*. 2005;44:10893–10904.
34. Ejendal KF, Hrycyna CA. Differential sensitivities of the human ATP-binding cassette transporters ABCG2 and P-glycoprotein to cyclosporin A. *Mol Pharmacol*. 2005;67:902–911.
35. Greenberger LM, Lisanti CJ, Silva JT, Horwitz SB. Domain mapping of the photo-affinity drug-binding sites in P-glycoprotein encoded by mouse mdr1 b. *J Biol Chem*. 1991;266:20744–20751.
36. Mosmann T. Rapid colorimetric assay for cellular growth and survival: application to proliferation and cytotoxicity assays. *J Immunol Methods*. 1983;65:55–63.